

Massive gluons and quarks and the equation of state obtained from SU(3) lattice QCD

Péter Lévai^{1,2} and Ulrich Heinz²

¹KFKI Research Institute for Particle and Nuclear Physics,
P. O. Box 49, Budapest, 1525, Hungary

²Institut für Theoretische Physik, Universität Regensburg,
D-93040 Regensburg, Germany

24 October 1997

Abstract

We analyze recent results of SU(3) lattice QCD calculations with a phenomenological parametrization for the quark-gluon plasma equation of state based on a quasi-particle picture with massive quarks and gluons. At high temperature we obtain a good fit to the lattice data using perturbative thermal quark and gluon masses from an improved HTL scheme. At temperatures close to the confinement phase transition the fitted masses increase above the perturbative value, and a non-zero (but small) bag constant is required to fit the lattice data.

1 INTRODUCTION

Strong interactions are described by SU(3) Yang-Mills field theory, and the fundamental degrees of freedom of Quantum Chromodynamics (QCD) are gluons and quarks. At high temperature this theory is weakly coupled, allowing for the use of perturbative methods. The leading order contributions to the characteristic collective excitations and the equation of state of a quark-gluon plasma were already determined many years ago [1, 2, 3]. A gauge invariant approach to non-leading corrections was derived more recently in form of the Hard Thermal Loop (HTL) approximation [4, 5, 6] and its improved versions [7, 8].

The theory of QCD predicts the appearance of a phase transition between the quark-gluon dominated high energy region and the hadronic state in the low energy region. The two states are characterized by a dramatic difference in the number of degrees of freedom. Perturbative QCD can describe successfully only the asymptotic state at very

high momenta, but it fails close to this phase transition where non-perturbative effects become dominant. Where the perturbative region begins is still a matter of debate [9]. The numerical method of lattice QCD can describe both sides of this phase transition. Recent developments of this field have yielded dramatic improvements both in the extrapolation to the continuum limit and for the inclusion of dynamical fermions.

The existence of this phase transition generated a large experimental effort to create it in the laboratory and investigate it in detail through heavy ion collisions. However, to verify the appearance of a deconfined state in such experiments we need accurate knowledge about its subsequent hadronization. There is a general interest to create phenomenological models for this phase transition which agree with the perturbative results at high energy and with the lattice QCD data at low energies. Such models must specify the basic degrees of freedom in the plasma state which will participate in the formation of hadrons during the confinement phase transition. The experience from phase transitions in solid state physics and other fields suggests the introduction of quasi-particles with effective masses generated through the interactions among the basic constituents. If a large part of the interaction can be included into the effective masses, then a quasi-particle description of the interacting matter can be generated in which the quasi-particles move freely or interact only weakly [10]. Such a model would be a preferable starting point for phenomenological hadronization models and for a description of the strongly interacting matter near the phase transition.

Our goal is to identify the appropriate degrees of freedom through an analysis of lattice QCD data. Similar attempts started as soon as good lattice QCD results on the equation of state of strongly interacting matter became available, and they developed in parallel with the improvements of the lattice data. It was observed already quite some time ago that the formula for the free energy density of a massive ideal gas gives a quite satisfactory description of the numerical lattice QCD simulations [11]. In Ref. [12] temperature dependent screening masses and coupling constants were extracted from SU(2) lattice data [13] and compared with perturbative results. In Ref. [14] it was shown that the obtained thermal mass can be indeed used as an effective mass in the equation of state, comparing favorably with SU(2) lattice QCD data. Early (very poor) lattice data on the pressure and energy density of pure SU(3) gauge theory in the temperature region $1.2 < T/T_c < 2.4$ [15] were interpreted with a constant gluon mass, $M_g \approx 500$ MeV, and a constant bag constant $B^{1/4} \approx 200$ MeV [16]. Newer SU(3) lattice data of better quality [17] made a reanalysis of the gluonic equation of state possible which yielded a new expression for the temperature dependent coupling constant in the thermal gluon mass [18]. A quasi-particle based, thermodynamically consistent analysis of the SU(2) [13] and SU(3) [17] lattice data was performed in Ref. [10] whose authors investigated in detail the temperature dependence of the thermal gluon mass and of the bag constant. New SU(3) lattice data with a complete continuum extrapolation appeared in Refs. [19, 20], and again a phenomenological analysis proved the applicability of an equation of state with massive gluons [21]. Furthermore it was shown [21] that at $T > 2.5 T_c$ the Debye screening mass extracted from lattice QCD correlation functions and the thermal gluon mass fitted to the lattice QCD equation of state are consistent with each other, such that at high temperature the perturbative QCD with effective massive degrees of freedom provides a good description of the lattice QCD results [21]. In Ref. [21] the lattice data fit

yielded $d = 17.2$ gluon degrees of freedom, supporting the presence of massive *transverse* modes only. A direct investigation of the screening mass in SU(3) lattice calculations was performed in Ref. [22] on both sides of the phase transition.

A somewhat different analysis of pure SU(3) lattice data was presented in Ref. [17]. It assumes the existence of massless gluons above a certain minimal momentum (“cut-off model”) together with glueball-like non-perturbative massive excitations. This model could reproduce the SU(3) lattice data quite well [17, 23].

All of the above analyses were performed for the case of pure SU(2) and SU(3) gauge theories, because sufficiently high-quality lattice QCD data existed only in these cases (for SU(3) the latest results can be found in Refs. [19, 20]). However, new lattice data including dynamical fermions appeared recently, with $N_f = 2$ [24, 25] and $N_f = 4$ [26] quark flavors. Extended investigations are under evaluation for the cases $N_f = 1, 3, 6$ and $N_f \geq 7$ (see Ref. [27]), but in their present state they can not yet be used to extract temperature dependent thermal masses. These new lattice results can now be used for the extraction of a phenomenological equation of state for the quark-gluon plasma (QGP) containing massive gluons and quarks, which to our knowledge has not been published elsewhere. Similar work is under way in the group of A. Peshier and B. Kämpfer [28].

The understanding of the dynamical generation of effective quark and gluon masses could be very important in many research fields. Dynamical mass generation is an essential ingredient for the solution of the infrared catastrophe in hot gauge theories [29] and the formulation of effective field theoretical approaches to thermal QCD [30]. It is at the heart of recent new approximation schemes such as the “screened perturbation theory” [31, 32]. Screening masses have also successfully been used to regulate the low- p_T behavior in the parton cascade approach to ultrarelativistic heavy ion collisions [33]. Massive quarks are the basic degrees of freedom in hadronization models: the phenomenological model ALCOR is based on the coalescence of massive quarks and antiquarks into hadrons [34]; transport descriptions of the hadronization based on the Nambu-Jona-Lasinio model contain massive quarks as well [35]. Massive quarks and gluons obtained from HTL approximation [6] were already applied to estimate charm production at RHIC and LHC energies [36].

In Sec. 2 we summarize the present knowledge about the thermal and screening masses in perturbative thermal QCD. In Sec. 3 we overview the equation of state of quasi-particles, its most important thermodynamical properties and discuss the criterium of thermodynamical consistency. In Sec. 4 we analyze pure SU(3) lattice QCD results; we determine the relevant number of gluonic degrees of freedom, the temperature dependent gluon mass and coupling constant, the temperature dependent bag constant and investigate the screening mass. In Sec. 5 we repeat this analysis on lattice data with $N_f = 2$ and $N_f = 4$ dynamical fermion species. In Sec. 6 we generate the equation of state of the QGP in general and investigate the speed of sound in this system. In Sec. 7 we include hadronic matter into our investigation and describe phenomenologically the phase transition between QGP and hadronic matter on the basis of our new equation of state obtained from lattice QCD data. In Sec. 8 we discuss our results.

2 THERMAL AND SCREENING MASSES IN PERTURBATIVE QCD

2.1 Gluons

There are essentially two ways to define an effective dynamical gluon mass: via the pole of the effective gluon propagator, or via the long-range behavior of the potential between two heavy color sources. In both cases one has to address the question of gauge invariance of the result for the mass, since the defining objects are not themselves gauge invariant.

On a perturbative level, it was noticed by Klimov [2] and Weldon [3] that the leading term in a high-temperature expansion of the 1-loop gluon polarization tensor was gauge invariant. It was later shown by Heinz [37] that the same result for the gluon polarization tensor could be obtained from classical color kinetic theory in the linear response approximation. From this expression for the polarization tensor Weldon [3] derived the following dispersion relation for transverse gluons with momenta $\omega, k \gg gT$:

$$\omega^2 = k^2 + M_{g,\infty}^2(T) , \quad (1)$$

$$M_{g,\infty}^2(T) = \frac{g^2 T^2}{2} \left(\frac{N_c}{3} + \frac{N_f}{6} \right) . \quad (2)$$

One might object that the high temperature limit in which the polarization tensor was obtained is inconsistent with the limit $\omega, k \gg gT$ under which Eq. (1) was derived. However, Rebhan et al. showed recently [7, 8] that the validity of Eq. (1) does not depend on the high temperature limit taken in Ref. [3]; indeed, near the light cone the transverse 1-loop polarization function is given by the gauge invariant result

$$\Pi_t(\omega^2 = k^2) = M_{g,\infty}^2(T) \quad (3)$$

independent of the magnitude of $\omega = k$ relative to T . Since for large momenta $k \gg gT$ the gluon dispersion relation moves arbitrarily close to the light cone, $M_g(T)$ can be interpreted as the thermal gluon mass in the high momentum limit. Its inclusion as a gluon mass term in higher orders of perturbation theory removes certain classes of collinear singularities near the light cone, and within the context of Hard Thermal Loop resummation [4, 5, 6] it leads to the so-called “improved HTL resummation scheme” [8].

The “Debye screening mass” M_D , on the other hand, is related to the behavior of gluonic excitations at small momenta. It can be defined either through the static limit of the gluon polarization tensor $\Pi_{\mu\nu}(\omega = 0, k)$ for $k \rightarrow 0$ or via the behavior of the potential between two heavy color charges at large distances, $V(r) \sim \exp(-M_D r)/r$ [6]. In the first case a gauge invariant result can be obtained from the leading term of the high temperature expansion for the 1-loop gluon polarization operator [2, 3] or, equivalently, from the 1-loop result within the HTL resummation scheme [4, 5, 6] for the gluon polarization operator at momenta $\omega, k < gT$. In the second case, care must be taken to make the external sources gauge invariant [6].

In the HTL approximation one obtains from the behavior of

$\Pi_L(\omega = 0, k \rightarrow 0)$ the Debye mass [4, 5, 38]

$$M_D^2 = 2M_{g,\infty}^2(T) = g^2 T^2 \left(\frac{N_c}{3} + \frac{N_f}{6} \right) . \quad (4)$$

This result is related to the 1-loop plasmon frequency, ω_p , obtained from the gluon dispersion relation (pole of the propagator) for $k \rightarrow 0$, by $M_D^2 = 3\omega_p^2$.

2.2 Quarks

Similarly to the gluon propagator, one can study the quark propagator in the 1-loop approximation. In the high temperature or low-momentum limit $\omega, k \ll T$ [2, 3] or, equivalently, in the HTL approximation [4, 5] one obtains

$$M_f^2(T) = \frac{N_c^2 - 1}{2N_c} \frac{g^2 T^2}{8} = \frac{g^2 T^2}{6} . \quad (5)$$

This can be interpreted as the effective quark mass for soft quarks with momenta $\omega, k < gT$. For high momenta $\omega, k \gg gT$ the fermion dispersion relation again approaches the light cone, and one can make use of the gauge invariant light cone limit of the 1-loop fermion self energy [8]:

$$\Sigma_f(\omega^2 = k^2) = M_{f,\infty}^2(T) , \quad (6)$$

$$M_{f,\infty}^2(T) = 2M_f^2(T) = \frac{g^2 T^2}{3} . \quad (7)$$

Again this is an exact 1-loop result, independent of the value of $\omega = k$, and $M_{f,\infty}$ can be interpreted as the thermal quark mass for high momentum quarks, $k \gg gT$.

2.3 Temperature dependent coupling constant

The thermal gluon and quark masses obtained from perturbative QCD are displayed in Eqs. (2) and (7). All masses depend on the temperature T and the strong coupling constant g . At higher orders of the loop expansion, the coupling g begins to run as a function of T , giving rise to a temperature dependent effective coupling constant $g(T)$. In $SU(N_c)$ gauge theory at $T = 0$, in the presence of N_f quark flavors the 1-loop expression for the running coupling constant as a function of the momentum transfer Q is

$$g^2(Q^2) = \frac{48\pi^2}{(11N_c - 2N_f) \ln(-Q^2/\Lambda_N^2)} . \quad (8)$$

Here Λ_N is the cut-off parameter. It was shown in Ref. [39] that in a thermal system it makes sense to introduce a temperature dependent function $g^2(T)$ by the following parametrization:

$$g^2(T) = \frac{48\pi^2}{(11N_c - 2N_f) \ln F^2(T, T_c, \Lambda)} . \quad (9)$$

We expect $F(T, T_c, \Lambda)$ to be linear in the region where perturbation theory is valid [39]. In other words, writing

$$F(T, T_c, \Lambda) = K(T/T_c) \cdot \frac{T}{T_c} \cdot \frac{T_c}{\Lambda_{\overline{MS}}} \quad (10)$$

we expect $K(T/T_c)$ to be a constant in the perturbative region, i.e. at high T . At low T a possible T -dependence of K reflects non-perturbative corrections.

In SU(3) at different N_f we have different critical temperatures T_c and different normalization parameters $T_c/\Lambda_{\overline{MS}}$ [40]:

$$\text{SU}(3), N_f = 0 \longrightarrow T_c = 260 \text{ MeV}; \quad \frac{T_c}{\Lambda_{\overline{MS}}} = 1.03 \pm 0.19 ; \quad (11)$$

$$\text{SU}(3), N_f = 4 \longrightarrow T_c = 170 \text{ MeV}; \quad \frac{T_c}{\Lambda_{\overline{MS}}} = 1.05 . \quad (12)$$

For $N_f = 2$ the critical temperature in SU(3) was determined as $T_c = 140 \text{ MeV}$ [24, 25], but the normalization factor $T_c/\Lambda_{\overline{MS}}$ is not known by the authors. From Eqs. (11) and (12) we will estimate this value by interpolation and we will use $T_c/\Lambda_{\overline{MS}} = 1.03$.

We will try to fit the lattice data with a non-interacting gas of massive quarks and gluons, with masses given by the perturbative expressions (2) and (7), but with g^2 replaced by a phenomenological running coupling $g^2(T)$. Using Eqs. (9) and (10) we can then extract a function $K(T/T_c)$. In a very early work [12] in pure SU(3) gauge theory this function $K(T/T_c)$ was determined from a similar fit to the heavy quark-antiquark potential; the fit result was a constant, $\hat{K}(T/T_c) = 19.0$. However, the authors of Ref. [12] used $T_c/\Lambda_{\overline{MS}} = 1.78 \pm 0.03$ which differs strongly from the now accepted value. With our normalization (11), $\hat{K}(T/T_c) = 19.0$ would correspond to $K(T/T_c) = 33.8$.

Another result was obtained recently from a numerical fit of the equation of state in pure SU(3) gauge theory [21]:

$$F(T, T_c, \Lambda) = 4.17 \frac{T}{T_c} - 2.96 . \quad (13)$$

Obviously, this parametrization differs from Eq. (10).

Our expectation is to obtain a constant $K(T/T_c)$ function in that temperature region where perturbative QCD and the quasi-particle picture of the lattice QCD results overlap. A strong temperature dependence of $K(T/T_c)$ implies non-perturbative effects. We summarize our results on the function $K(T/T_c)$ for different values of N_f in Sects. 4 and 5.

3 EQUATION OF STATE WITH QUASI-PARTICLES

In this Section we introduce the equation of state of a pure gluon plasma and a quark-gluon plasma consisting of massive quasi-particles. This equation of state (resp. its parameters)

will be determined from the SU(3) lattice data. The key point is to consider temperature dependent effective masses, $M_i(T)$, which are dynamically generated. We can introduce the dispersion relation for quasi-particles:

$$\omega_i^2(k) = k^2 + M_i^2(T) . \quad (14)$$

Here k is the momentum of the quasi-particle and $\omega_i(k)$ is its energy. A pure gluon plasma contains only gluons ($i = g$, $N_f = 0$), a QGP consists of quarks and antiquarks also ($i = g, q, \bar{q}$, $N_f > 0$). We can define the Bose or Fermi distribution functions $f_i(k)$ for the quasi-particles as

$$f_i(k) = [\exp\{\sqrt{k^2 + M_i^2(T)}/T\} \pm 1]^{-1} = [\exp(\omega_i/T) \pm 1]^{-1} . \quad (15)$$

In addition to the effective masses $M_i(T)$ we also need the effective number of degrees of freedom of the quasi-particles to determine pressure and energy density. The correct value for the number of effective gluonic degrees of freedom is not obvious, since a massless vector boson has two helicity states, but massive vector bosons have three spin states. One possibility is to introduce a temperature dependent effective degeneracy factor $D(T)$ for the gluons. We will determine the value of $D(T)$ in a pure gluon plasma ($N_f = 0$), where quark degrees of freedom do not interfere. Later we can assume the same value for $D(T)$ in a QGP.

Another possibility is to fix the number of gluonic degrees of freedom (e.g. at its perturbatively expected value $D_g = 16$) as well as the number of quark and antiquark degrees of freedom. In this case we have the freedom to introduce an effective interaction term for those contributions of the strong interaction which can not be absorbed by the presence of effective masses. We parametrize this term by a temperature dependent “bag constant”, $B(T)$. This interaction term $B(T)$ can be determined in a pure gluon plasma as well as in a quark-gluon plasma. As we will see in the following Section, in the QGP phase quarks and anti-quarks will also contribute to $B(T)$, so its physical meaning differs from the bag constant parameter of the MIT Bag Model; nevertheless we will use the same notation for convenience.

3.1 The number of effective gluonic degrees of freedom $D(T)$

Let us first consider pure SU(3) gauge theory where we wish to find out the number of contributing gluonic quasi-particle degrees of freedom, $D(T)$. A strongly interacting gluon plasma contains not only the transverse gluon modes, but at low momenta $k < gT$ there exist also longitudinal plasma excitations. It was shown in Ref. [4] that at high momenta $k \gg gT$ the longitudinal modes disappear, in the sense that the residue of the corresponding pole in the propagator becomes exponentially small. Since the equation of state is dominated by particles with momenta $k \sim T$, we expect at high temperatures $T \rightarrow \infty$ (where g becomes small) the contribution of the longitudinal modes to be negligible. On the other hand, at low temperatures (where g can become of order 1 or larger) their contribution may be relatively large. Therefore we can not a priori neglect them from the analysis of lattice QCD data.

We will introduce a temperature dependent effective number of gluon degrees of freedom $D(T)$, generalizing the approach of Ref. [18] where D was taken as a constant (temperature independent) fit parameter. We expect that in the high temperature limit there are only transverse gluonic quasi-particle modes, yielding $D(T = \infty) = D_g = 16$. At low temperatures the longitudinal gluons are expected to also contribute, giving $D(T) > D_g$.

With these assumptions the thermodynamical pressure $P_g(T)$ of pure gluon matter (which is nothing but the grand canonical thermodynamical potential) can be written as

$$P_g(T) = \frac{D(T)}{(2\pi)^3} \int_0^\infty d^3k \frac{k^2}{3\omega_g(k)} f_g(k) . \quad (16)$$

From the thermodynamic identity

$$\varepsilon(T) = T \cdot \frac{dP(T)}{dT} - P(T) \quad (17)$$

(we work at zero net baryon density, $\mu_B = 0$) one obtains the following relation for the energy density:

$$\varepsilon_g(T) = \frac{D(T)}{(2\pi)^3} \int_0^\infty d^3k \omega_g(k) f_g(k) + W_D(T) , \quad (18)$$

$$W_D(T) = T \frac{P_g(T)}{D(T)} \frac{dD(T)}{dT} - T M_g(T) \frac{dM_g(T)}{dT} \frac{D(T)}{(2\pi)^3} \int_0^\infty \frac{d^3k}{\omega_g(k)} f_g(k) . \quad (19)$$

Here $W_D(T)$ summarizes the extra terms stemming from the temperature derivative of the effective mass and effective number of degrees of freedom. On the other hand, a consistent quasi-particle picture demands $W_D \equiv 0$ [10]. Requiring this identity yields a differential equation for $D(T)$:

$$D(T) = D(T^*) + \int_{T^*}^T dT' M_g(T') \frac{dM_g(T')}{dT'} \frac{3D(T')}{\int_0^\infty \frac{d^3k}{\omega_g(k)} \frac{k^2}{\omega_g(k)} f_g(k)} . \quad (20)$$

Here T^* is an integration constant. If the functions $M_g(T)$ and $D(T)$ satisfy this selfconsistency condition, then we have a thermodynamically consistent quasi-particle description.

Lattice calculations yield numerical values for the functions $P_g(T)$ and $\varepsilon_g(T)$. These two sets of data are sufficient to determine for each value of T the quantities $M_g(T)$ and $D(T)$ such that they satisfy Eqs. (16-19) with $W_D = 0$. Since the lattice results were created in a thermodynamically consistent way we expect that the resulting functions $M_g(T)$ and $D(T)$ will satisfy Eq. (20). We will check this as a test for the consistency of our extraction procedure for $M_g(T)$ and $D(T)$. Our numerical results on $M_g(T)$ and $D(T)$ will be summarized in Sec. 4.

3.2 The temperature dependent interaction term $B(T)$

We can also investigate the high temperature limit from another point of view [10, 21]. Let us fix the value of the gluonic degrees of freedom at every temperature to $D(T) \equiv D_g = 16$,

assuming that only transverse gluons contribute to the thermodynamic quantities, and calculate directly any extra contribution to the pressure and the energy density. In this way both pure gluon matter and a quark-gluon plasma can be investigated. We will here consider a QGP with N_f quark flavors and the usual number of quark degrees of freedom: $D_q = D_{\bar{q}} = 2 \cdot 3 \cdot N_f = 6N_f$.

The effective quark mass $M_q(T)$ will be related to the effective gluon mass $M_g(T)$ through the value of the temperature dependent coupling constant $g(T)$ via the perturbative expressions in Eqs. (2) and (7) for the effective masses. This means that we absorb non-perturbative features into a common non-perturbative fit function $g(T)$, without touching the perturbative form of the Eqs. (2) and (7) itself.

The deviation of $\varepsilon_0(T) = \sum_i \varepsilon_i(T)$ and $P_0(T) = \sum_i P_i(T)$ from the ideal gas values corresponding to the effective masses $M_i(T)$ and the fixed degeneracy factors D_g , D_q and $D_{\bar{q}}$ will be parametrized by a temperature dependent function $B(T)$. At high temperature, where we expect a perturbative picture based on free quarks and transverse gluons to be valid, $B(T)$ should vanish. At lower temperature, $B(T)$ provides another measure for non-perturbative physics which can not be absorbed into effective quark and gluon masses. Both quarks and gluons contribute to $B(T)$.

We introduce $B(T)$ by writing the pressure in the form

$$P(T) = \sum_{i=g,q,\bar{q}} \frac{D_i}{(2\pi)^3} \int_0^\infty d^3k \frac{k^2}{3\omega_i(k)} f_i(k) - B(T) , \quad (21)$$

motivated by the MIT Bag Model. Thermodynamic identities yield the following relation for the energy density:

$$\varepsilon(T) = \sum_{i=g,q,\bar{q}} \frac{d_i}{(2\pi)^3} \int_0^\infty d^3k \omega_i(k) f_i(k) + B(T) + \widetilde{W}_B(T) . \quad (22)$$

Here $\widetilde{W}_B(T)$ summarizes the extra terms obtained from the temperature derivative of $B(T)$ and of the effective mass $M_i(T)$. Similarly as above thermodynamic consistency of our quasi-particle model requires $\widetilde{W}_B(T) \equiv 0$. This yields to the following integral representation for $B(T)$ [10, 21]:

$$B(T) = B(T^*) - \sum_{i=g,q,\bar{q}} \frac{D_i}{(2\pi)^3} \int_{T^*}^T dT' M_i(T') \frac{dM_i(T')}{dT'} \int_0^\infty \frac{d^3k}{\omega_i} f_i(k) . \quad (23)$$

Again T^* is an integration constant. If this expression is satisfied by the functions $M_i(T)$ and $B(T)$, we have a thermodynamically correct quasi-particle description containing effective gluons and quarks with effective thermal masses.

Similarly as above, from the numerical values for the functions $P(T)$ and $\varepsilon(T)$ obtained from lattice QCD and assuming $\widetilde{W}_B(T) = 0$, we can determine the appropriate values for $M_i(T)$ (resp. $g(T)$) and $B(T)$ through Eqs. (21) and (22). As before we expect that the obtained functions $M_i(T)$ and $B(T)$ will satisfy Eq. (23). Once again this is a good numerical consistency check for our extraction of the functions $M_i(T)$, $B(T)$.

4 ANALYSIS OF LATTICE DATA FOR PURE SU(3) GAUGE THEORY

We analyze the latest lattice data in the continuum limit for pure SU(3) gauge theory [19, 20]. The calculations of Ref. [19] show a $\pm 2\%$ error on the data for $P(T)$, $\varepsilon(T)$ and $s(T)$. We include this error into our analysis; it will be indicated in Figs. 1, 2 and 3 by dotted lines above and below the solid lines corresponding to the results extracted from the mean values.

We begin by determining the effective number of gluonic quasi-particle degrees of freedom in a gluon plasma, extracting the functions $M_g(T)$ and $D(T)$ as explained in Sec. 3.1. Fig. 1a shows the temperature dependent effective gluon mass, $M_g(T)$, while in Fig. 1b we display the effective number of gluonic degrees of freedom, $D(T)$. At high temperature, $T > 2.3 T_c$, the number of degrees of freedom is rather constant, $D(T) = 14.5 \pm 1$. Please note that the $\pm 2\%$ error of the lattice data results in an uncertainty of about 1 gluon degree of freedom. Within this uncertainty the result is surprisingly close to the naive expectation that at high temperature only the transverse gluonic modes are present. In the low temperature region, $T < 2.3 T_c$, the function $D(T)$ increases, which one may wish to associate with the increasing contribution of the longitudinal modes. However, for $T < 1.5 T_c$, $D(T)$ rises very strongly and exceeds even the value of 24 expected for massive gluons with 8 color and 3 helicity states. This indicates the presence of strong non-perturbative effects at low temperature not all of which can be absorbed by the effective gluon mass. In fact, part of the strong rise in $D(T)$ is driven by the strong increase of the effective gluon mass which leads to exponential suppression of the thermodynamical contributions to $P(T)$ and $\varepsilon(T)$. We consider this behavior of $D(T)$ as physically unreasonable and believe that a parametrization of these non-perturbative effects via an extra interaction term makes more sense.

To this end we fix the effective number of gluonic modes to $D_g = 16$ as suggested by the behavior of $D(T)$ in Fig. 1b and our perturbative prejudice at large T . This means that we consider only transverse effective gluons as quasi-particle states and subsume all further interaction effects into a non-perturbative “bag constant” $B(T)$. The procedure is described in Sec. 3.2. Fig. 2a shows the temperature dependent transverse gluon mass $M_g(T)$ resulting from this approach. Comparing with Fig. 1a one sees that at large values of T the effective mass is now somewhat larger, compensating for the choice of a fixed $D_g = 16$ instead of the best fit value $D_g \approx 14.5$ in Fig. 1b. For smaller temperatures, however, the rise of $M_g(T)$ is much weaker than in Fig. 1a, and $M_g(T)$ also shows a much weaker sensitivity to the statistical error of the lattice data on $P(T)$ and $\varepsilon(T)$. This indicates that this type of parametrization provides a more reasonable fit to the lattice data than the one above in terms of $M_g(T)$ and $D(T)$. Please note that the effective gluon masses shown in Fig. 2a correspond in the region $T > 2 T_c$ to a coupling constant $g = \sqrt{2} M_g(T)/T \approx 1.3 - 1.4$, in agreement with other extraction procedures: for example, the authors of Ref. [41] obtained from the interquark potential at small distances the value $\alpha \approx 0.15$ which translates into $g = 1.37$.

Fig. 2b shows the function $B(T)/\varepsilon(T)$, the interaction term relative to the total

energy density. At high temperatures, $T > 2.3 T_c$, the bag constant is very small, only about 2–3% of the total energy density, although slightly negative. We take the smallness of $B(T)$ as confirmation for the validity of a quasi-particle picture at large temperature. Near $T = 2.3 T_c$ $B(T)$ changes sign, increasing for smaller values of T , but never exceeding a value of 15% of the total energy density even at T_c . Note that this relatively small deviation from an ideal quasi-particle picture gave rise to the dramatic and unphysical behavior of $D(T)$ (and $M_g(T)$) in the alternative approach above. Clearly, the parametrization via $B(T)$ is more economical and leads to a more selfconsistent picture.

The dashed line in Fig. 2b shows the result of an integration of Eq. (23), using the extracted $M_g(T)$ from Fig. 2a and choosing boundary conditions $B(T^*) = 0$ at $T^* = 2.3 T_c$. The agreement with the numerically extracted values for $B(T)$ is nearly perfect indicating the thermodynamical consistency of the lattice data and our extraction procedure.

From the temperature dependent gluon mass, $M_g(T)$, one can determine the temperature dependent coupling constant, $g(T)$, and extract the function $K(T/T_c)$ given in Eq. (10). The result for pure SU(3) gauge theory is shown in Fig. 3. The dotted lines again indicate the $\pm 2\%$ systematic error of the lattice data. One can see that at high temperature we obtain a constant value, $K(T/T_c \rightarrow \infty) = 18 \pm 8$. At low temperature $K(T/T_c)$ decreases indicating a larger coupling constant and a larger thermal gluon mass. Close to the phase transition the function approaches the value $K(T/T_c \rightarrow 1) = 1.5$; the precise value depends, however, on the latent heat at the phase transition point which is still under intensive investigation in lattice QCD calculations.

The obtained curve can be fitted rather well with the following function (dashed line in Fig. 3):

$$K(T/T_c) = \frac{18}{18.4 \cdot e^{-0.5(T/T_c)^2} + 1}. \quad (24)$$

If we start from this approximate function of $K(T/T_c)$ for the coupling constant $g(T)$, we obtain an analytically parametrized, approximate thermal gluon mass $M_g(T)$ (see Eqs. (2,9,10)). Once we fix the boundary condition $B(T^*) = 0$ at $T^* = 2.3 T_c$ as determined from the numerical analysis of the lattice data (see Fig. 2b), the bag constant $B(T)$ can be uniquely reconstructed by integrating Eq. (23). With $M_g(T)$ and $B(T)$ known, $P(T)$ and $\varepsilon(T)$ are easily evaluated using Eqs. (21,22) (with $\widetilde{W}_B = 0$). This means that Eq. (24) together with the value for T^* provide a complete analytical parametrization of the equation of state. In Fig. 4 we compare the original lattice QCD data (diamonds) with the thus reconstructed values (dashed and dash-dotted lines). The dash-dotted lines neglect the interaction term $B(T)$ and thus represent only the quasi-particle contribution to P and ε . Clearly the agreement between the model and the lattice data is at most qualitative in this case. Including the bag term, however, (dashed lines) we obtain nearly perfect reproduction of the lattice data. Fig. 4 demonstrates the usefulness of a thermodynamically consistent quasi-particle picture. The deviation from the Stefan-Boltzmann values indicates that the massless degrees of freedom can not provide a satisfactory description, while the quasi-particle model plus bag term leads to qualitative improvements.

5 ANALYSIS OF SU(3) LATTICE DATA FOR $N_f = 2, 4$

Newest lattice calculations including dynamical fermions can be used to determine the equation of state for a realistic quark-gluon plasma including light quarks. The numerical lattice QCD results can be found in Refs. [24, 25] for $N_f = 2$ and in Ref. [26] for $N_f = 4$. Following these articles we interpolated the expected continuum result in both cases. From Ref. [24] for $N_f = 2$ we used the data for a current quark mass $am_q = 0.0125$ (octagons in Figs. 9 and 10 in Ref. [24] and circles in Fig. 7 here). The statistical error of the lattice data is small, $< 1\%$ for the pressure and $\approx 2 - 4\%$ for the energy density. From Ref. [26] for $N_f = 4$ we used the data set for a current quark mass $m_q/T = 0.2$ and we considered their extrapolation of the energy density to the chiral limit (see \square in Fig. 4 of Ref. [26] and in Fig. 7 here). In this case the statistical errors are even smaller, but the systematic errors resulting from the extrapolations to the chiral and continuum limits are hard to judge. To estimate the possible influence of errors on the lattice data for our extraction procedure we will consider a universal $\pm 2\%$ error in both cases; the corresponding uncertainty will be indicated by dotted lines in Figs. 5 and 6.

In the framework of perturbation theory the effects of dynamical quarks on the gluon dynamics are small and can be simply included into the thermal gluon mass and Debye screening length. No additional gluonic collective modes arise. However, at small momenta there are additional fermionic collective modes, the “plasminos” [6]. Based on our experience in pure gluodynamics they are not expected to contribute to the equation of state at high temperature; again the residues of their poles in the quark propagator vanish exponentially for moments $k \gg gT$ [4]. We will therefore assume a fixed number of degrees of freedom, given by the perturbative values at high T , $D_g = 16$, $D_q = D_{\bar{q}} = 6N_f$, and include all collective interaction effects into an interaction term $B(T)$ as for the purely gluonic system above.

The obtained results are qualitatively very similar to the previous ones for the purely gluonic case. Fig. 5a shows the obtained results for the effective gluon mass, M_g/T . Since $\frac{M_g(T)}{T} = \frac{g(T)}{\sqrt{2}} \sqrt{1 + \frac{N_f}{6}}$, Fig. 5a can be viewed as giving the temperature dependence of the effective coupling constant $g(T)$ which according to Eq. (7) also determine the effective quark mass. From Fig. 5 and Eq. (2) we extract $g \approx 1.6$ in the region $T > 2 T_c$ for $N_f = 4$, somewhat larger than for the purely gluonic case.

Fig. 5b shows the interaction term relative to the total energy density $B(T)/\varepsilon(T)$ both for $N_f = 2$ and $N_f = 4$. Similarly to the result in pure SU(3) gauge theory, the interaction term $B(T)$ remains small at $T > 2 - 2.3 T_c$, and does not exceed 15% of the energy density in the low temperature region. In the case $N_f = 2$ the lattice data allow us to extract $M_g(T)$ and $B(T)$ only in the temperature region $T_c < T < 1.4 T_c$, however the characteristics of the obtained curves are close to the results obtained for $N_f = 4$.

Fig. 6 displays the obtained functions $K(T/T_c)$ (solid lines) together with the expected errors (dotted lines) stemming from an assumed typical $\pm 2\%$ uncertainty in the lattice data. For all three cases, $N_f = 0, 2$ and 4 , the functions $K(T/T_c)$ are very similar

(within the admittedly large error bars). Within the existing uncertainties we can thus define a universal function $K(T/T_c)$; differences due to variations of N_c and N_f can be largely absorbed into T_c and $\Lambda_{\overline{MS}}$ in Eq. (10). It would be very interesting to see whether the existence of such a universal function $K(T/T_c)$ is confirmed by future higher quality lattice data.

Since the data for purely gluonic SU(3) span a much larger range than those including dynamical fermions, we will use the analytical form (24) extracted from the gluonic case also in our quasi-particle picture for the full QGP. For the zero point of $B(T)$ we will again choose the value $T^* = 2.3$ determined in the purely gluonic SU(3) case, although (modulo large numerical uncertainties) the $N_f \neq 0$ data seem to favor a somewhat smaller value.

For a QGP with $N_f = 2$ quark flavours Fig. 7a shows the lattice data (circles for pressure and energy density) and the reconstructed values for $\varepsilon(T)$ and $P(T)$, both including the bag constant (dashed lines) and neglecting the interaction term (dash-dotted lines). For $N_f = 4$ quark flavours the analogous quantities are displayed in Fig. 7b. Here the squares give directly the lattice data from Ref. [26] for the energy density, while the diamonds represent the continuous line for the pressure given in Fig. 2 of Ref. [26]. In each case inclusion of the interaction term $B(T)$ improves the picture. The agreement is weaker than in the pure SU(3) case (see Fig. 4), but the pressure is reproduced rather nicely as well as the energy density at high temperature. Note that here we used the function $K(T/T_c)$ from Eq. (24). The discrepancy in the region $T \approx T_c$ may be connected to the use of massive current quarks in the actual lattice simulations and associated uncertainties in the extrapolation to the chiral limit (for a discussion see Ref. [26]). In view of those the 10 – 15% discrepancy between the reconstructed curves and data is surprisingly small, especially if we remember that we used here the parametrization which was obtained from the pure SU(3) case.

6 SPEED OF SOUND IN THE MASSIVE QGP

In hydrodynamical models of strongly interacting matter the dynamical behavior is mostly determined by the value of the speed of sound:

$$c_s^2 = \frac{dP}{d\varepsilon} = \frac{dP/dT}{d\varepsilon/dT} . \quad (25)$$

Since the energy density $\varepsilon(T)$ was obtained from Eq. (17) we can rewrite this as

$$c_s^2 = \frac{(P + \varepsilon)/T}{d\varepsilon/dT} , \quad (26)$$

which is more directly connected to the lattice data. For a noninteracting ($B(T) = 0$) gas of massless particles the speed of sound is $c_s^2 = 1/3$. In Ref. [36], using Eq. (26), it was found that even for a non-interacting ($B(T) = 0$) massive quark-gluon gas the speed of sound remains very close to $c_s^2 = 1/3$. (In that work thermal masses from earlier HTL

calculations [6] and a running coupling constant according to Eqs. (9,10) with a constant $K(T/T_c)$ were used.) If there are, however, strong remaining interactions which cannot be absorbed in the masses but require a non-vanishing and possibly strongly T -dependent $B(T)$, this will generate deviations of c_s^2 from the ideal gas value, especially near T_c [42]. A strong drop of c_s^2 near T_c will give rise to a “soft point” in the equation of state at which the ability of the matter to generate expansion flow is minimal.

Since in our analysis the interaction term $B(T)$ remains small and changes smoothly with T , we expect only weak modifications of the speed of sound around T_c . Fig. 8 displays the speed of sound c_s^2 for $N_f = 0, 2, 4$ in our quasi-particle picture and confirms this expectation. Including the bag term $B(T)$ (dashed lines), $c_s^2 \approx 0.33$ in the high temperature limit, and c_s^2 decreases to a minimum value $c_{s,0}^2|_{min} = 0.15$ around T_c . If we neglect the interaction term $B(T)$ and calculate the speed of sound $c_{s,0}^2$ from the expression

$$c_{s,0}^2 = \frac{dP_0}{d\varepsilon_0} = \frac{dP_0(T)/dT}{d\varepsilon_0(T)/dT}, \quad (27)$$

where $P_0(T) = P(T) + B(T)$ and $\varepsilon_0(T) = \varepsilon(T) - B(T)$, then (see dash-dotted line in Fig. 8) the speed of sound shows only a very weak temperature dependence, decreasing from $c_{s,0}^2 \approx 0.30$ at $T = 4.5 T_c$ to $c_{s,0}^2|_{min} = 0.23$ at T_c . If we instead use Eq. (26) also in this case (as in Ref. [36]), where $B(T)$ cancels in the numerator, then the resulting speed of sound is very close to the full result (dashed line), because of the small influence of $B(T)$ on the energy density in the denominator of Eq. (26). Our result agrees with the calculations in Ref. [36] in the high temperature region and differs around T_c because of the non-linear behavior of $K(T/T_c)$ indicating non-perturbative effects.

These results on the speed of sound show that a massive quark-gluon plasma will expand rapidly and that therefore the phase transition should be a fast process without detectable duration effects. Even where the pressure already shows large ($> 50\%$) deviations from the massless ideal gas law, the speed of sound still deviates by less than 10% from the value $1/\sqrt{3}$. In this way our analysis of lattice QCD results favors fast hadronization models [34, 43, 44] of the deconfined phase.

7 GLUON SUPPRESSION AROUND T_c IN SU(3) GAUGE THEORY

In this Section we investigate some phenomenological consequences of the large effective quark and gluon masses. Fig. 9 displays the effective masses in GeV for $N_f = 0, 2, 4$. All masses behave similarly, since they are connected to each other by the function $K(T/T_c)$ in the effective coupling constant $g(T)$. Just above the critical temperature the effective masses drop, but then they remain rather constant in the temperature region $1.2 T_c < T < 2.5 T_c$. The mass values for the case $N_f = 2$ are smaller than for $N_f = 0$ due to the smaller critical temperature $T_c = 140$ MeV instead of 260 MeV. For $N_f = 4$ they increase again due to the larger contribution from quark loops and the somewhat larger $T_c = 170$ MeV. The gluon masses are large in the cases $N_f = 0, 4$, of order $M_g = 650 - 750$ MeV in

the temperature region $T_c < T < 3 T_c$ (solid lines). In the same temperature region the quark masses are of order $M_q = 300 - 400$ MeV (dashed lines).

Large effective masses yield smaller number density at the same energy density. Thus the density of these massive quasi-particles will be smaller than in the massless case. Fig. 10 demonstrates this by displaying the density ratio of the massive quasi-particles and the massless ones, n_i/n_i^0 (solid lines for gluons and dotted lines for quarks) as a function of temperature. At large temperature the ratio flattens and eventually approaches 1, but close to the critical temperature the ratio drops very quickly to values much smaller than 1. This indicates that the massive quark-gluon plasma is much more dilute than a massless QGP, especially near T_c .

Now we compare the abundances of quarks and gluons relative to each other. Eqs. (2) and (7) imply that in our model the gluon effective mass is always larger than the quark effective mass by the ratio

$$\frac{M_{g,\infty}}{M_{q,\infty}} = \sqrt{\frac{3}{2} \left(\frac{N_c}{3} + \frac{N_f}{6} \right)}, \quad (28)$$

which even increases with the number of quark flavor N_f . Each gluon degree of freedom will thus be suppressed compared to each quark degree of freedom. After multiplying the corresponding degeneracy factors we can compute the density ratio for gluons

$$R_g = \frac{n_g}{n_g + n_q + n_{\bar{q}}}, \quad (29)$$

which is shown in Fig. 11 as a function of T . The horizontal lines show the ratio R_g^0 for the massless QGP. The deviation caused by the effective mass is clearly seen, and a considerable suppression of the relative gluon number occurs near the phase transition. Near T_c , for $N_f = 2$ we have $R_g = 0.25$ which means that only 25% of the particles are gluons while the remaining 75% are quarks and antiquarks. For $N_f = 4$ the gluon suppression is even stronger and near T_c we find only 10% gluons and 90% quarks and anti-quarks.

These results show that the massive QGP is a dilute system dominated by massive quarks and antiquarks. Gluons are much heavier than quarks and their number densities are suppressed. These properties indicate that lattice QCD results support the formation of a quark-antiquark dominated plasma state just above the critical temperature, which contains mostly massive quarks and antiquarks. This system hadronizes quickly. Fast hadronization is also favored by the fact that the effective quark masses are already close to the masses in the “constituent quark” picture of hadrons. Clusterization of these massive quarks leads directly to multiquark states with similar masses as those of the finally observed hadrons, allowing for immediate hadron formation without having to wait for further energy transfer.

8 CONCLUSIONS

Lattice data in pure SU(3) gauge theory and new lattice results with $N_f = 2$ and $N_f = 4$ dynamical fermions suggest that beyond the phase transition temperature strong non-perturbative effects dominate the deconfined state. In order to understand this phenomenon and to facilitate the application of lattice results in dynamical descriptions of the evolution of the deconfined phase and its hadronization we analyzed the lattice data in a phenomenological model assuming the appearance of massive quasi-particles, namely massive quarks and massive transverse gluons. We determined a temperature dependent effective coupling constant $g(T)$, which determines the effective masses, and the interaction term $B(T)$, which summarizes contributions not to be included into the effective masses. We found that such a quasi-particle picture works very well. The interaction term $B(T)$ remains small and the extracted dynamical mass is consistent with perturbative QCD results at high temperature while it includes non-perturbative contributions at low temperature. In all cases, $N_f = 0, 2, 4$, the obtained characteristics are very similar. If we determine $g(T)$ in the purely gluonic case and extend it in an appropriate way for $N_f > 0$, we can reproduce approximately the $N_f = 2, 4$ lattice data. This fact suggest the existence of a universal description of non-perturbative effects in the fermionless and fermionic cases. Our analysis leads to a thermodynamically consistent quasi-particle model for the QGP equation of state which is parametrized via an effective coupling constant $g(T)$ through Eqs. (9,10,24) and the zero point T^* of the interaction term $B(T)$. Further lattice data with improved quality over a wider temperature region are needed to fix $g(T)$ and T^* more accurately.

The successful reproduction of lattice data by this quasi-particle model indicates the validity of such an approximation. The consequences of the appearance of these quasi-particles are very interesting: near T_c lattice results indicate the existence of a QCD phase which is dominated by massive quarks and anti-quarks, while the even heavier gluons are suppressed. This quark-antiquark plasma can be characterized by a relatively large speed of sound which indicates fast dynamical evolution and the lack of long time delays during hadronization. Massive quarks and anti-quarks can form clusters, 2- and 3-body objects, which can be easily associated with the hadronic mass spectra: massive quarks ($M_q = 300 - 350$ MeV) above the critical temperature turn into similarly massive “constituent quarks” inside hadrons below T_c in a smooth but rapid hadronization process.

ACKNOWLEDGMENTS

Discussions with T.S. Biró, E. Laermann, B. Müller, A. Schäfer, M. Thoma, J. Zimányi, and especially with B. Kämpfer and A. Peshier, are gratefully acknowledged. P.L. is grateful for the warm hospitality of the Institute für Theoretische Physik at Universität Regensburg. This work was supported in part by DAAD by the National Scientific Research Fund (Hungary) OTKA Grant Nos. F019689 and T016206 (P.L.), and by DFG, BMBF and GSI (U.H.).

References

- [1] J. Kapusta, Nucl. Phys. **B148** (1979) 461.
- [2] V.V. Klimov, Zh. Eksp. Teor. Fiz. **82** (1982) 336 (Sov. Phys. JETP **55** (1982) 199).
- [3] H.A. Weldon, Phys. Rev. **D26** (1982) 1394; **D26** (1982) 2789.
- [4] R.D. Pisarski, Physica **A158** (1989) 146.
- [5] J. Frenkel and J.C. Taylor, Nucl. Phys. **B334** (1990) 199;
E. Braaten and R.D. Pisarski, Nucl. Phys. **B337** (1990) 569.
- [6] M. Le Bellac, *Thermal Field Theory* (Cambridge University Press, Cambridge, England, 1996);
M. H. Thoma, hep-ph/9503400.
- [7] R. Baier, S. Peigne, and D. Schiff, Z. Phys. **C62** (1994) 337;
F. Flechsig, A.K. Rebhan, and H. Schulz, Phys. Rev. **D52** (1995) 2994;
U. Krämmer, A.K. Rebhan, and H. Schulz, Ann. Phys. **238** (1995) 286.
- [8] U. Krämmer, M. Kreuzer, and A.K. Rebhan, Ann. Phys. **201** (1990) 223;
F. Flechsig and A.K. Rebhan, Nucl. Phys. **B464** (1996) 279.
- [9] K. Kajantie, M. Laine, J. Peisa, A. Rajantie, K. Rummukainen, and M. Shaposhnikov, Phys. Rev. Lett. **79**, 3130 (1997).
- [10] M.I. Gorenstein and S.N. Yang, Phys. Rev. **D52** (1995) 5206.
- [11] F. Karsch, Z. Phys. **C38** (1988) 147;
F. Karsch, Nucl. Phys. (Proc. Suppl.) **B9** (1989) 357.
- [12] F. Karsch, M.T. Mehr, and H. Satz, Z. Phys. **C37** (1988) 617.
- [13] J. Engels, J. Fingberg, K. Redlich, H. Satz, and M. Weber, Z. Phys. **C42** (1989) 341.
- [14] V. Goloviznin and H. Satz, Z. Phys. **C57** (1993) 671.
- [15] A. Ukawa, Nucl. Phys. **A498** (1989) 227c.
- [16] T.S. Biró, P. Lévai, and B. Müller, Phys. Rev. **D42** (1990) 3078.
- [17] J. Engels, J. Fingberg, F. Karsch, D. Miller, and M. Weber, Phys. Lett. **B252** (1990) 625.
- [18] A. Peshier, B. Kämpfer, O.P. Pavlenko, and G. Soff, Phys. Lett. **B337** (1994) 235.
- [19] G. Boyd, J. Engels, F. Karsch, E. Laermann, C. Legeland, M. Lütgemeier, and B. Petersson, Phys. Rev. Lett. **75** (1995) 4169; Nucl. Phys. **B469** (1996) 419.
- [20] E. Laermann, Nucl. Phys. **A610** (1996) 1c.

- [21] A. Peshier, B. Kämpfer, O.P. Pavlenko, and G. Soff, Phys. Rev. **D54** (1996) 2399.
- [22] B. Grossman, S. Gupta, U.M. Heller, and F. Karsch, Nucl. Phys. **B417** (1994) 289.
- [23] D.H. Rischke, M.I. Gorenstein, A. Schäfer, H. Stöcker, and W. Greiner, Phys. Lett. **B278** (1992) 19;
D.H. Rischke, J. Schaffner, M.I. Gorenstein, A. Schäfer, H. Stöcker, and W. Greiner, Z. Phys. **C56** (1992) 325.
- [24] C. Bernard, T. Blum, C. DeTar, S. Gottlieb, K. Rummukainen, U.M. Heller, J.E. Hetrick, D. Toussaint, L. Kärkkäinen, R.L. Sugar, and M. Wingate, Phys. Rev. **D55** (1997) 6861.
- [25] S. Gottlieb, U.M. Heller, A.D. Kennedy, S. Kim, J.B. Kogut, C. Liu, R.L. Renken, D.K. Sinclair, R.L. Sugar, D. Toussaint, and K.C. Wang, Phys. Rev. **D55** (1997) 6852.
- [26] J. Engels, R. Joswig, F. Karsch, E. Laermann, M. Lütgemeier, and B. Petersson, Phys. Lett. **B396** (1997) 210.
- [27] LATTICE'95 Conf., Nucl. Phys. (Proc. Suppl.) **B47** (1996);
LATTICE'96 Conf., Nucl. Phys. (Proc. Suppl.) **B53** (1997).
- [28] B. Kämpfer, O.P. Pavlenko, A. Peshier, M. Hentschel, and G. Soff, FZR-189 (1997), J. Phys. **G** in print.
- [29] E. Braaten, Phys. Rev. Lett. **74** (1995) 2164.
- [30] E. Braaten and A. Nieto, Phys. Rev. **D51** (1995) 6990.
- [31] F. Karsch, A. Patkós, and P. Petreczky, Phys. Lett. **B401** (1997) 69.
- [32] I.T. Drummond, R.R. Horgan, P.V. Landshoff, and A. Rebhan, hep-ph/9708426.
- [33] K.J. Eskola, B. Müller, and X.N. Wang, Phys. Lett. **B374** (1996) 20.
- [34] T.S. Biró, P. Lévai, and J. Zimányi, Phys. Lett. **B347** (1995) 6;
J. Zimányi, T.S. Biró, T. Csörgő, and P. Lévai, Heavy Ion Phys. **4** (1996) 55.
- [35] P. Rehberg, S.P. Klevansky, and J. Hüfner, Phys. Rev. **C53** (1996) 410.
- [36] P. Lévai and R. Vogt, Phys. Rev. **C56** (1997) in press, (hep-ph/9704360)
- [37] U. Heinz, Ann. Phys. **168** (1986) 148.
- [38] A.K. Rebhan, Phys. Rev. **D48** (1993) 3967.
- [39] K. Kajantie and J. Kapusta, Ann. Phys. **160** (1985) 477.
- [40] J. Fingberg, U. Heller and F. Karsch, Nucl. Phys. **B392** (1993) 493.
- [41] C. Michael and the UKQCD Coll., Nucl Phys. **B** (Proc. Suppl.) **30** (1993) 509;
G.S. Bali and K. Schilling, Nucl. Phys. **B** (Proc. Suppl.) **30** (1993) 513.

- [42] D. H. Rischke and M. Gyulassy, Nucl. Phys. **A597** (1996) 701; Nucl. Phys. **A608** (1996) 479.
- [43] T. Csörgő and L.P. Csernai, Phys. Lett. **B333** (1994) 494;
L.P. Csernai and I. Mishustin, Phys. Rev. Lett. **74** (1995) 5005.
- [44] J. Letessier, A. Tounsi, U. Heinz, J. Sollfrank, and J. Rafelski, Phys. Rev. **D51** (1995) 3408.

Figure Caption

- Fig. 1:** The temperature dependent effective gluon mass, $M_g(T)$, in units of temperature T (a) and the effective number of gluonic quasi-particle degrees of freedom, $D(T)$ (b) in pure SU(3) gauge theory ($N_f=0$) as a function of T/T_c . The horizontal line in Fig. 1b indicates $D_g = 16$.
- Fig. 2:** The temperature dependent effective gluon mass, $M_g(T)$, in units of temperature T (a) and the interaction term $B(T)$ normalized by the energy density $\varepsilon(T)$ (b) for pure SU(3) gauge theory ($N_f=0$) as a function of T/T_c . For details see text.
- Fig. 3:** The function $K(T/T_c)$ for the effective coupling constant $g(T)$ in pure SU(3) gauge theory. The solid line shows the mean values, the dotted lines show the influence of a $\pm 2\%$ systematic error of the lattice data on the function $K(T/T_c)$. The fitted function Eq. (24) is denoted by the dashed line, and the horizontal line at $K = 18$ indicates its asymptotic value.
- Fig. 4:** Lattice data for pure SU(3) gauge theory on ε/T^4 and $3P/T^4$ (diamonds) [19], their reconstruction with a free quasi-particle picture with $B(T) = 0$ (dash-dotted lines), and including the interaction term $B(T)$ (dashed lines). The horizontal line at 5.24 indicates the Stefan-Boltzmann value for massless non-interacting particles.
- Fig. 5:** The temperature dependent effective gluon mass, $M_g(T)$, in units of temperature T (a) and the interaction term $B(T)$ normalized by the energy density $\varepsilon(T)$ (b) in SU(3) gauge theory for $N_f=2$ and $N_f=4$ as a function of T/T_c .
- Fig. 6:** The function $K(T/T_c)$ from the effective coupling constant $g(T)$ in SU(3) gauge theory $N_f = 0, 2, 4$ (solid lines) and the influence of $\pm 2\%$ systematic error of lattice data on the function $K(T/T_c)$.
- Fig. 7:** SU(3) lattice data (symbols) and our model reconstruction (lines): $N_f = 2$ [24] (a) and $N_f = 4$ [26] (b). The reconstructed quantities are denoted by dash-dotted lines in a simple quasi-particle picture and dashed lines if the interaction term $B(T)$ is included. Horizontal lines indicate the Stefan-Boltzmann values for massless non-interacting particles, 12.17 and 19.08, respectively.
- Fig. 8:** The speed of sound c_s^2 , calculated for $N_f = 0, 2, 4$. The dash-dotted lines denote the results $c_{s,0}^2$ from the free quasi-particle model ($B(T) = 0$) while the dashed lines with asymptotic value $c_s^2 = 0.33$ indicate the results including the interaction term $B(T)$. Note that the differences between $N_f = 0, 2$ and 4 are hardly visible.
- Fig. 9:** The effective masses of quarks (dashed curves) and gluons (solid curves) in SU(3) gauge theory with $N_f=0, 2$ and 4 quark flavour.
- Fig. 10:** The density ratios between massive (n_i) and massless (n_i^0) quarks and gluons in SU(3) gauge theory for $N_f=0, 2$ and 4 .
- Fig. 11:** The relative gluon density $R_g = n_g/(n_g + n_q + n_{\bar{q}})$ for massive, R_g^0 for massless particles in $N_f = 2$ (solid lines) and in $N_f = 4$ (dashed lines) QGP.

Fig.1. SU(3), $N_f=0$ --- $M_g(T)/T$, $D(T)$

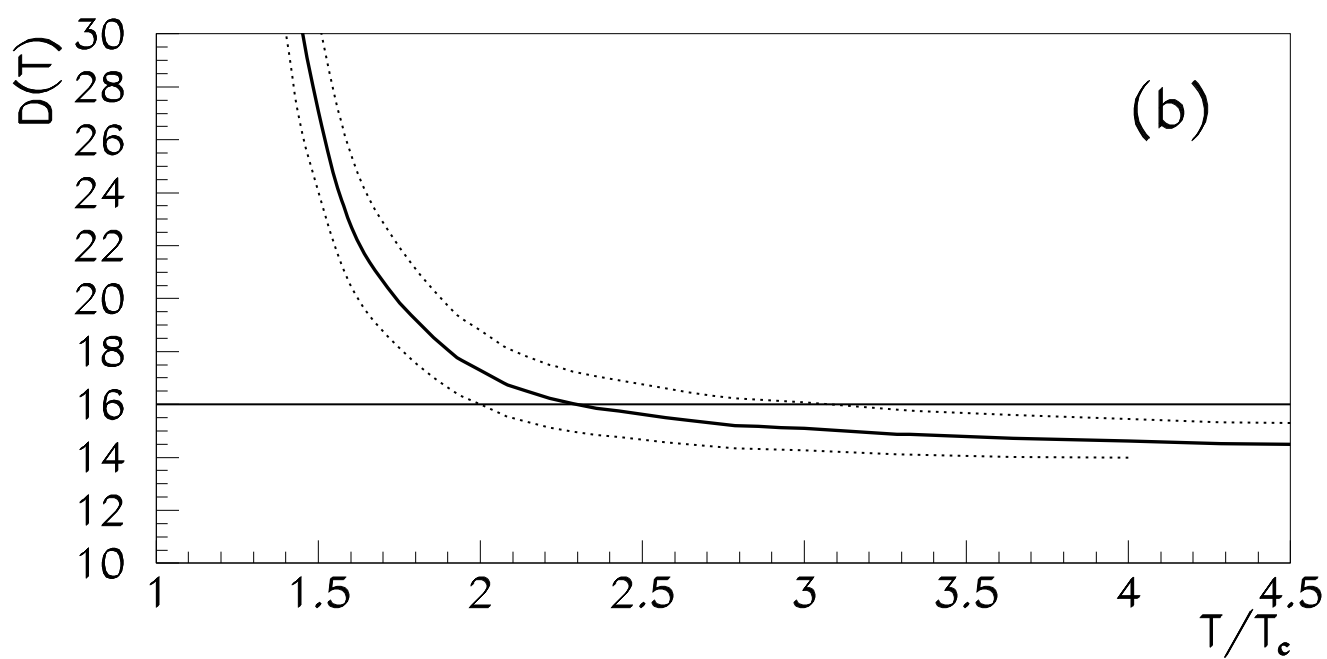
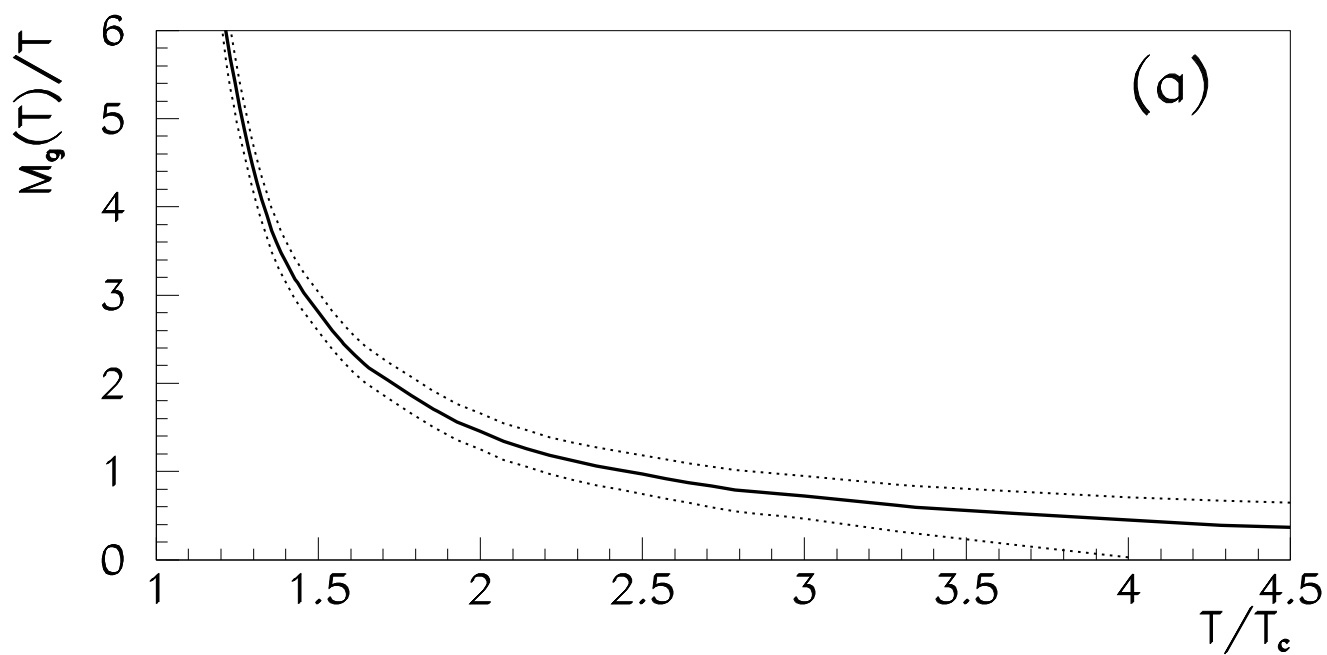


Fig.2. SU(3), $N_f=0$ --- $M_g(T)/T$, $B(T)/\varepsilon(T)$

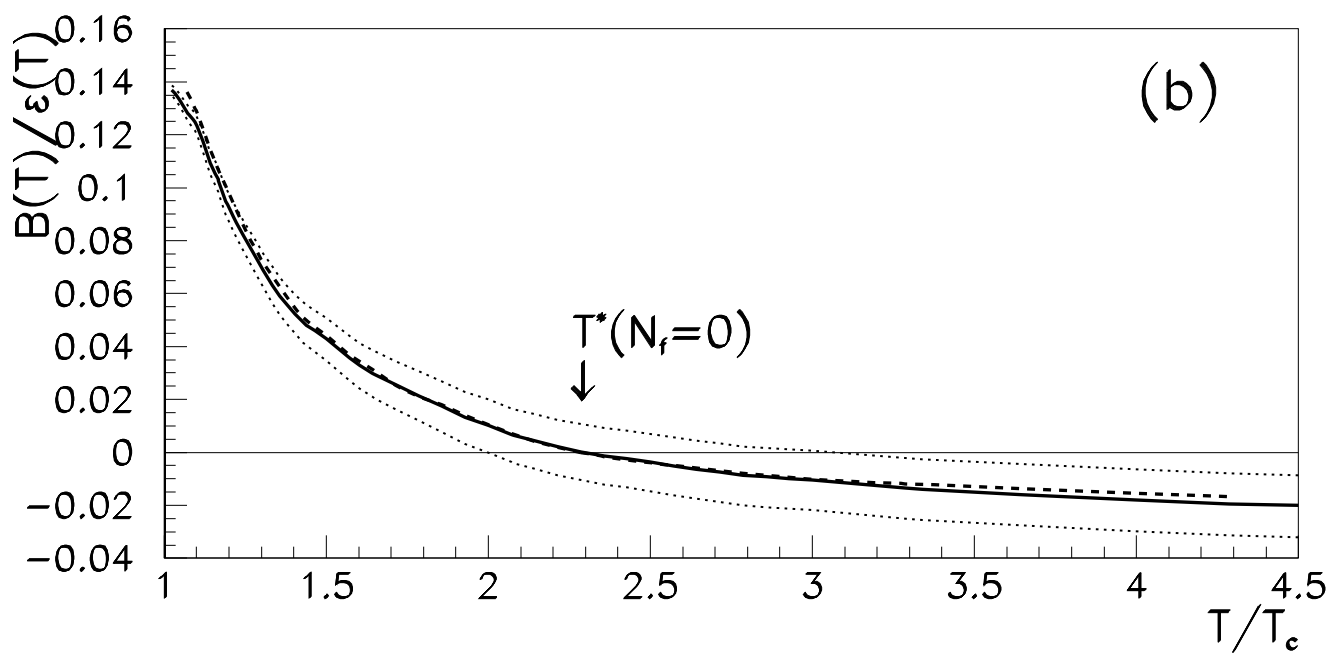
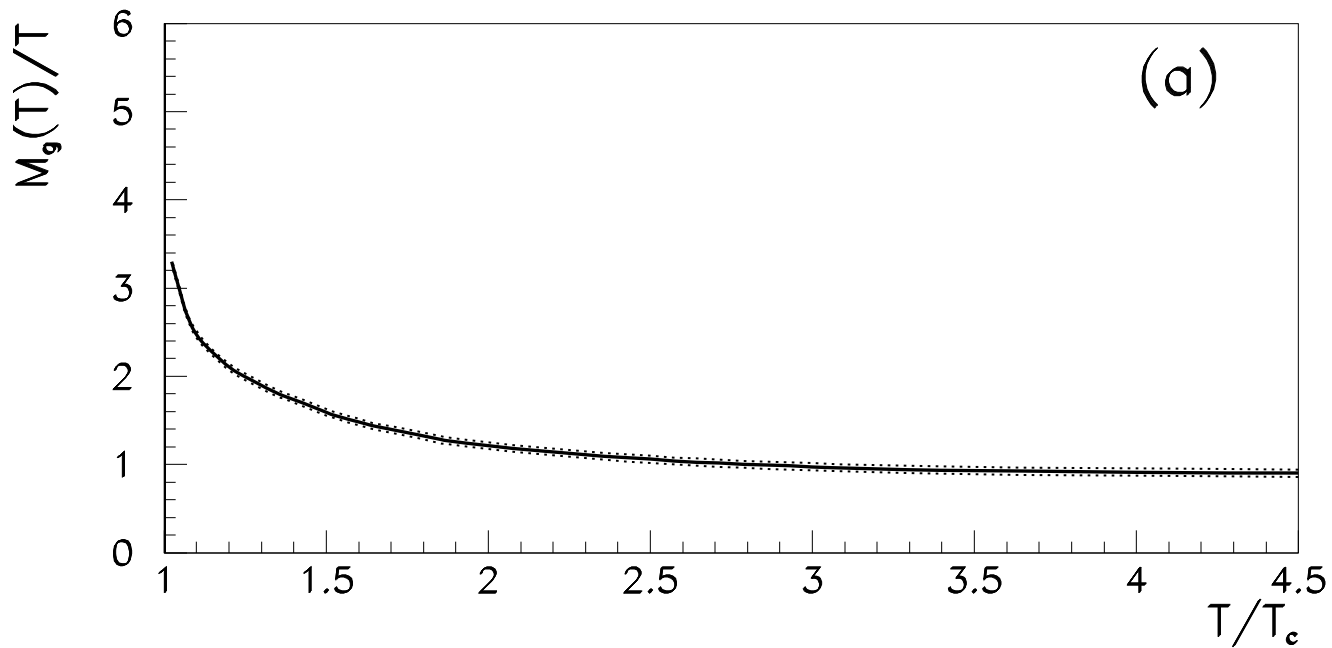


Fig.3. SU(3), $N_f=0$ --- $K(T/T_c)$

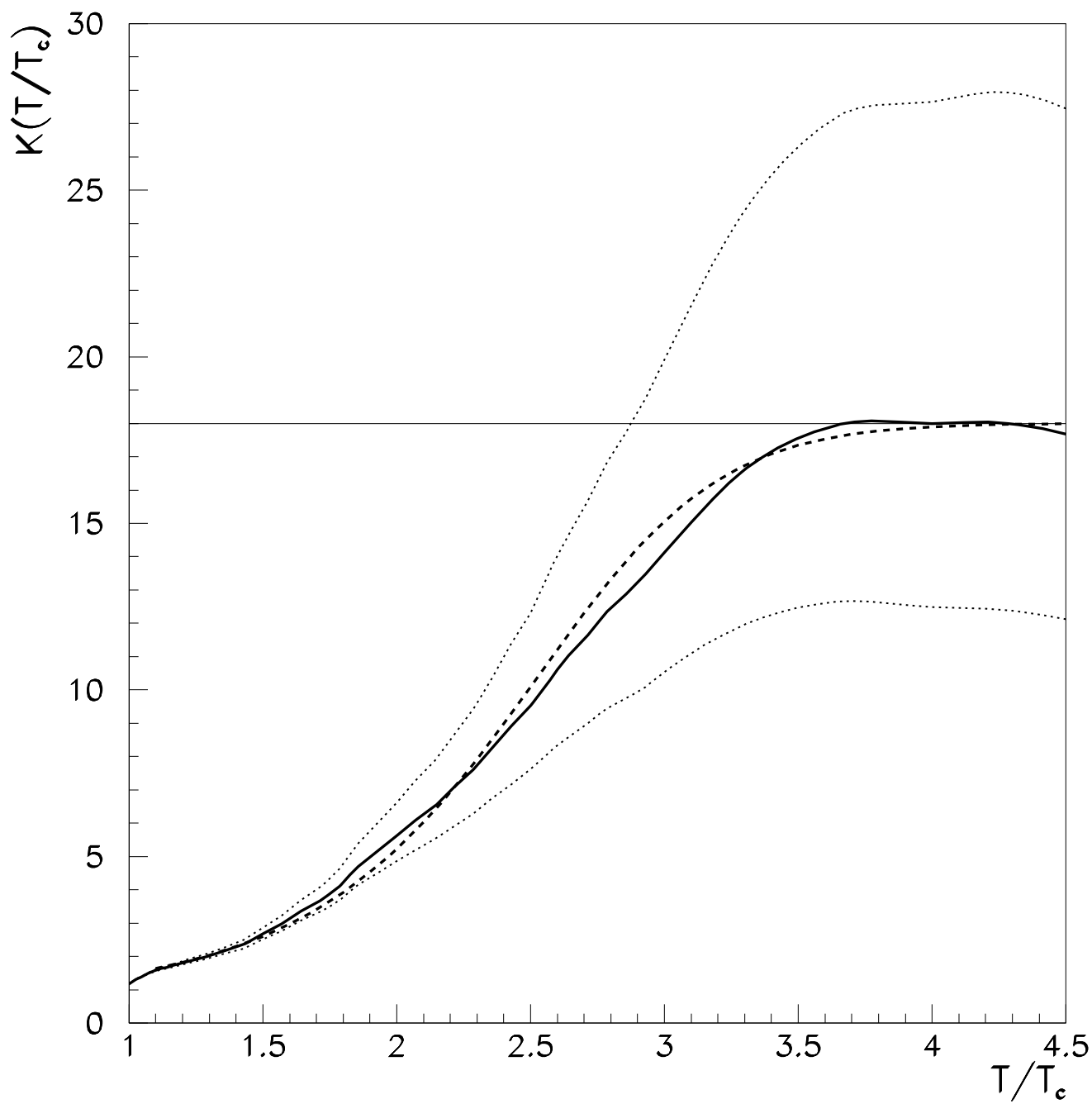


Fig.4. SU(3), $N_f=0$ --- EOS + Lattice QCD data

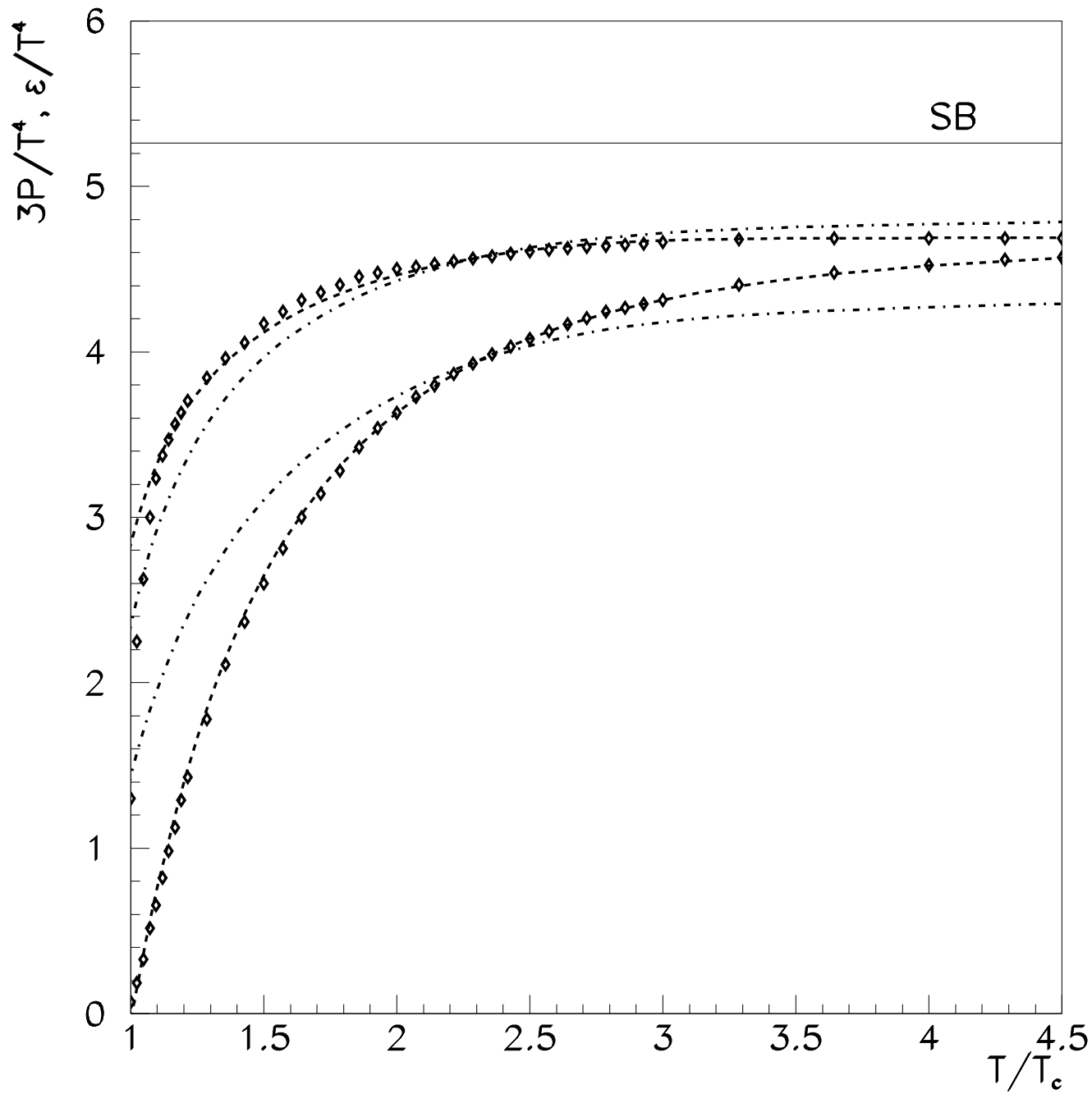


Fig.5. SU(3), $N_f=2,4$ --- $M_g(T)/T$, $B(T)/\varepsilon(T)$

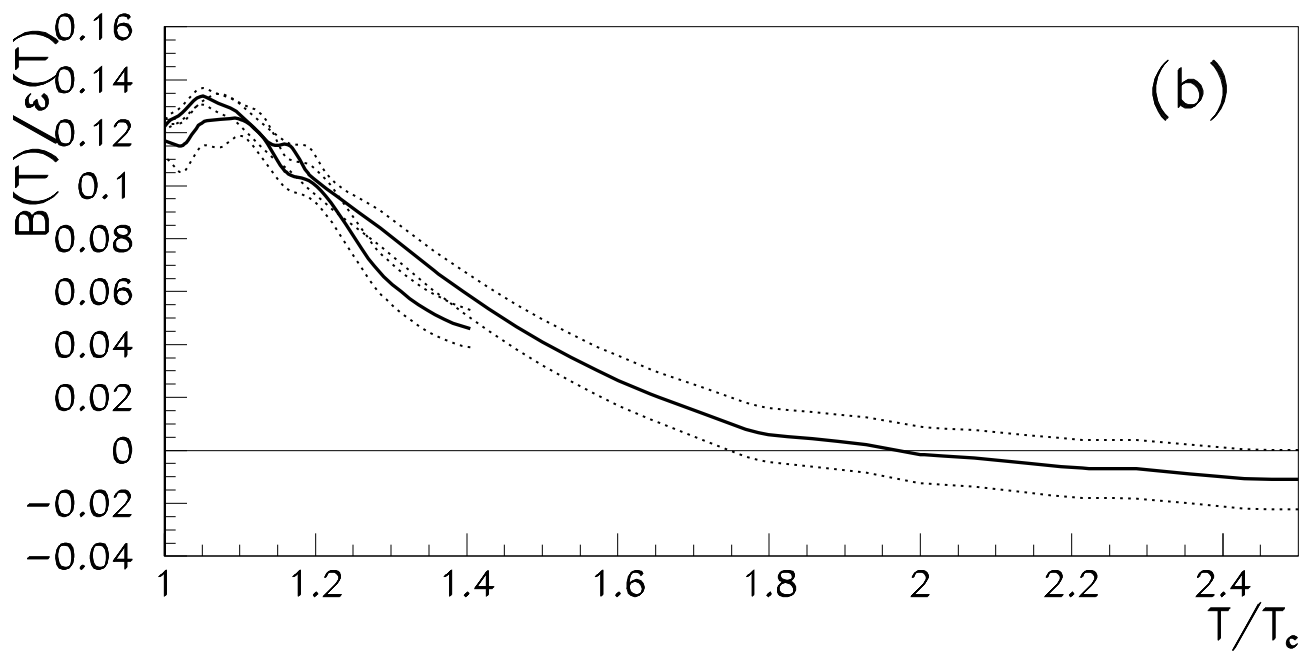
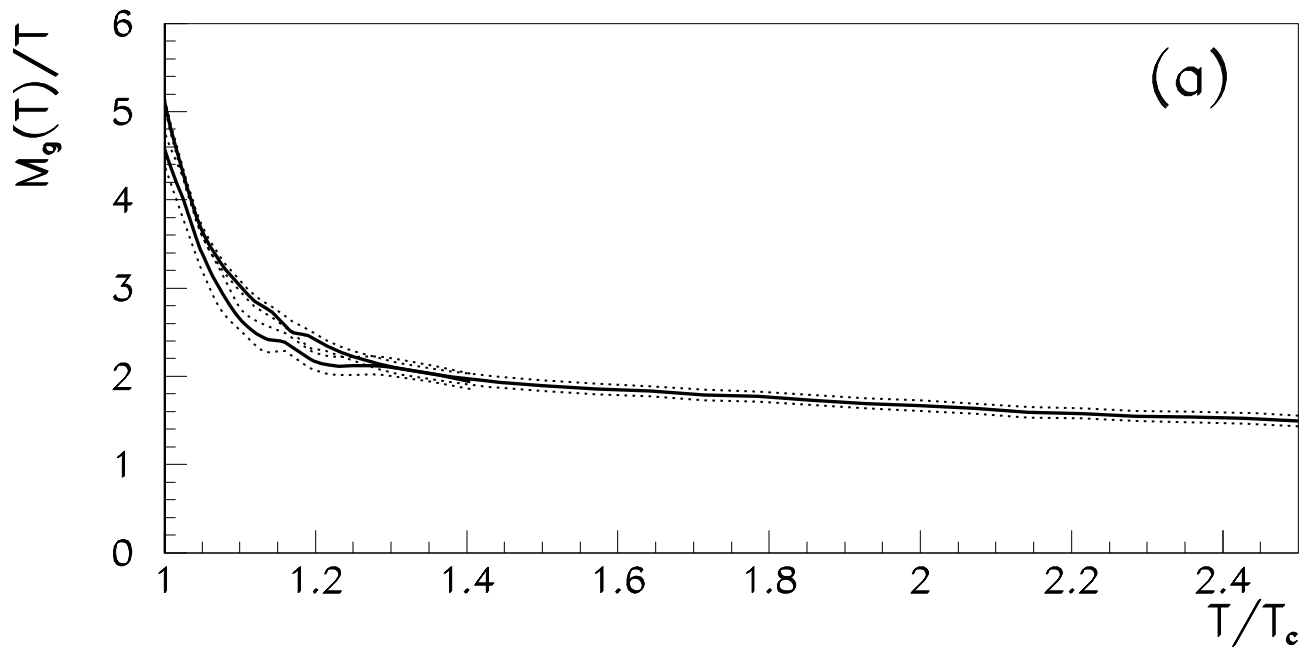


Fig.6. SU(3), $N_f=0,2,4$ --- $K(T/T_c)$

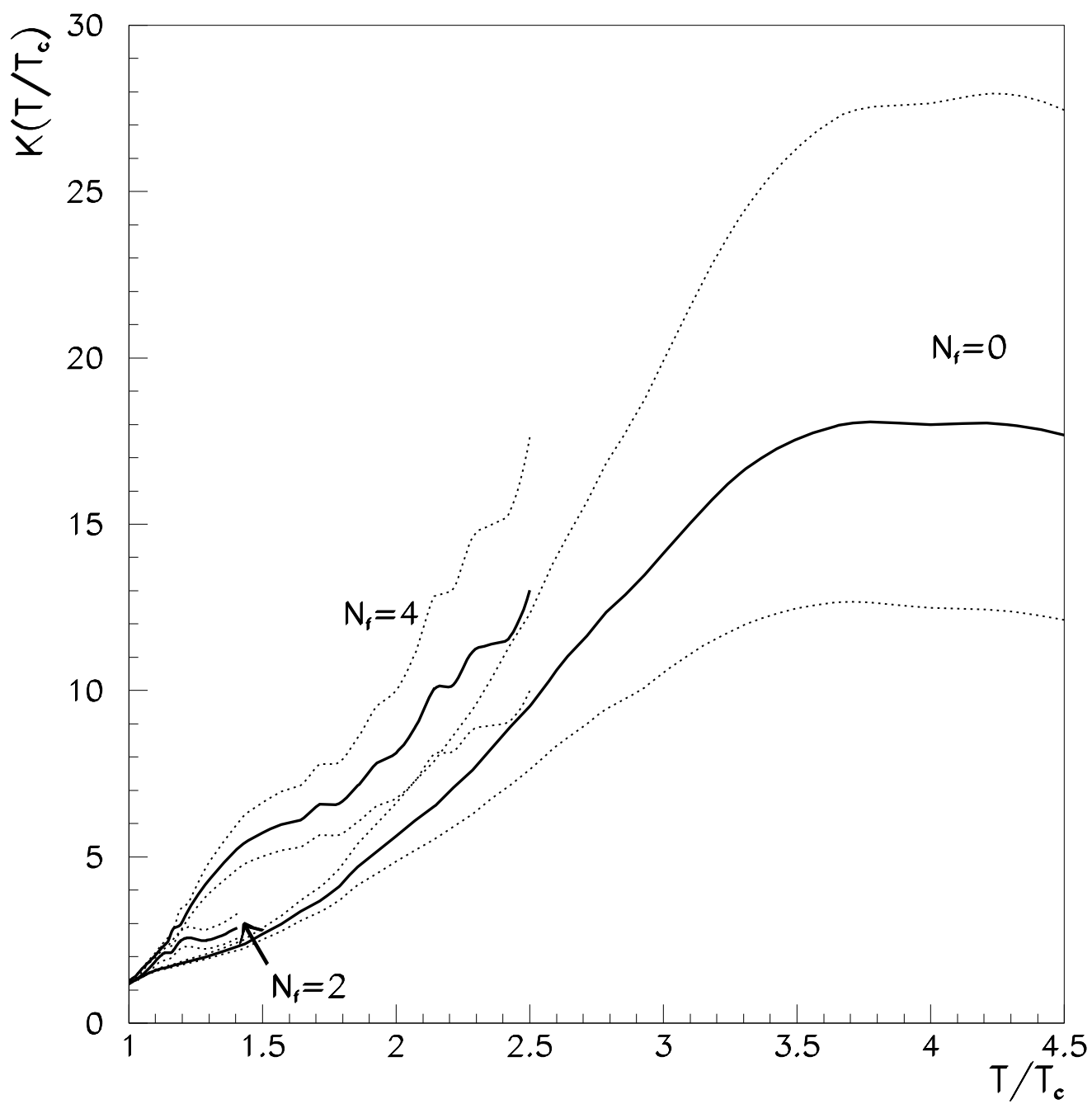


Fig.7. SU(3), $N_f=2,4$ --- EOS + Lattice QCD data

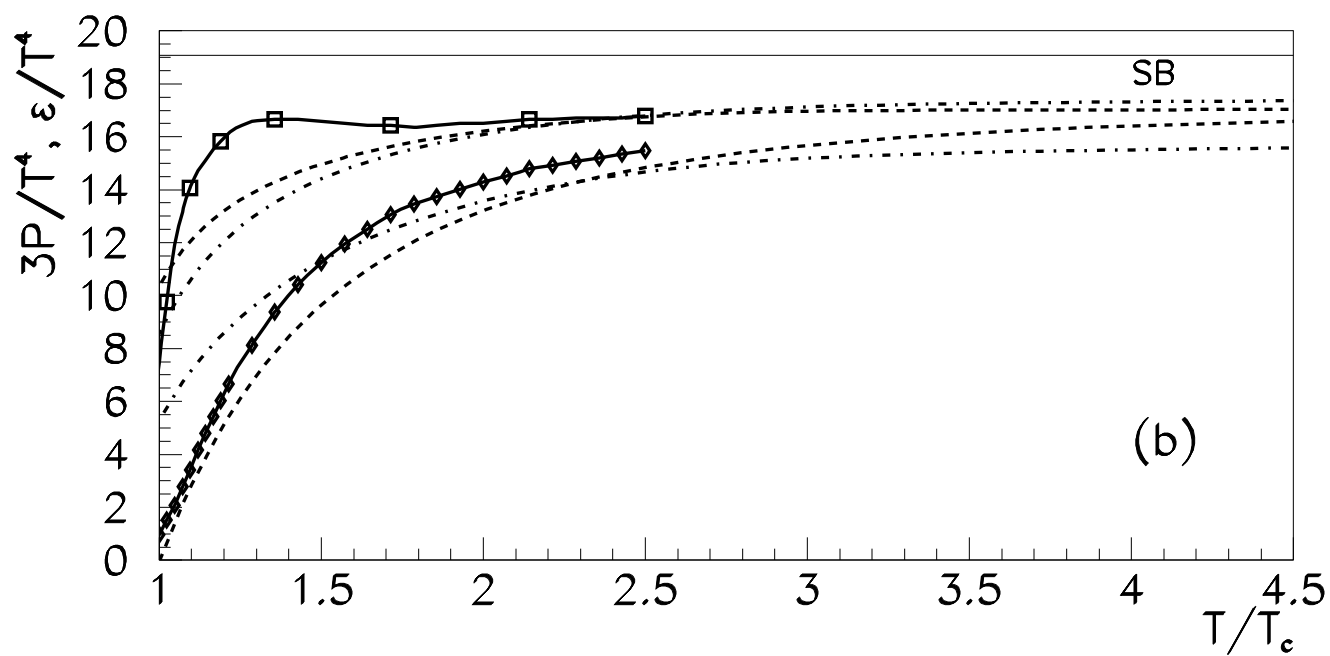
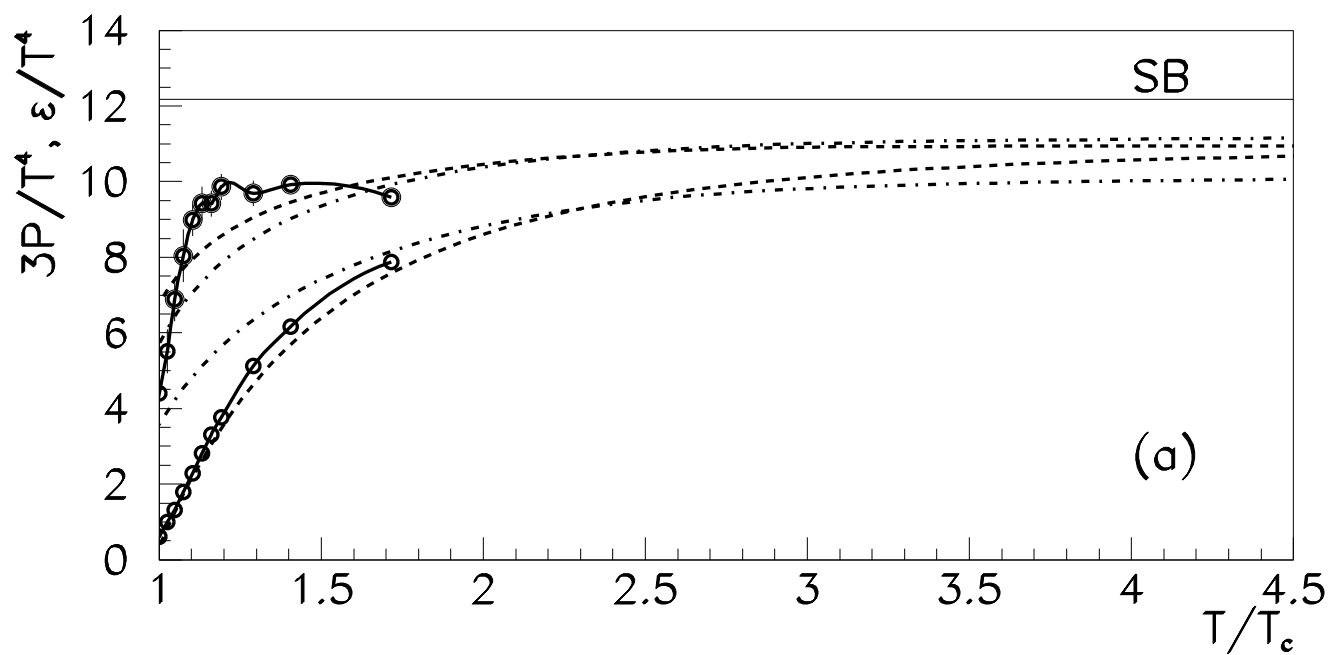


Fig.8. SU(3), $N_f=0,2,4$ --- $c_s^2, c_{s,0}^2$

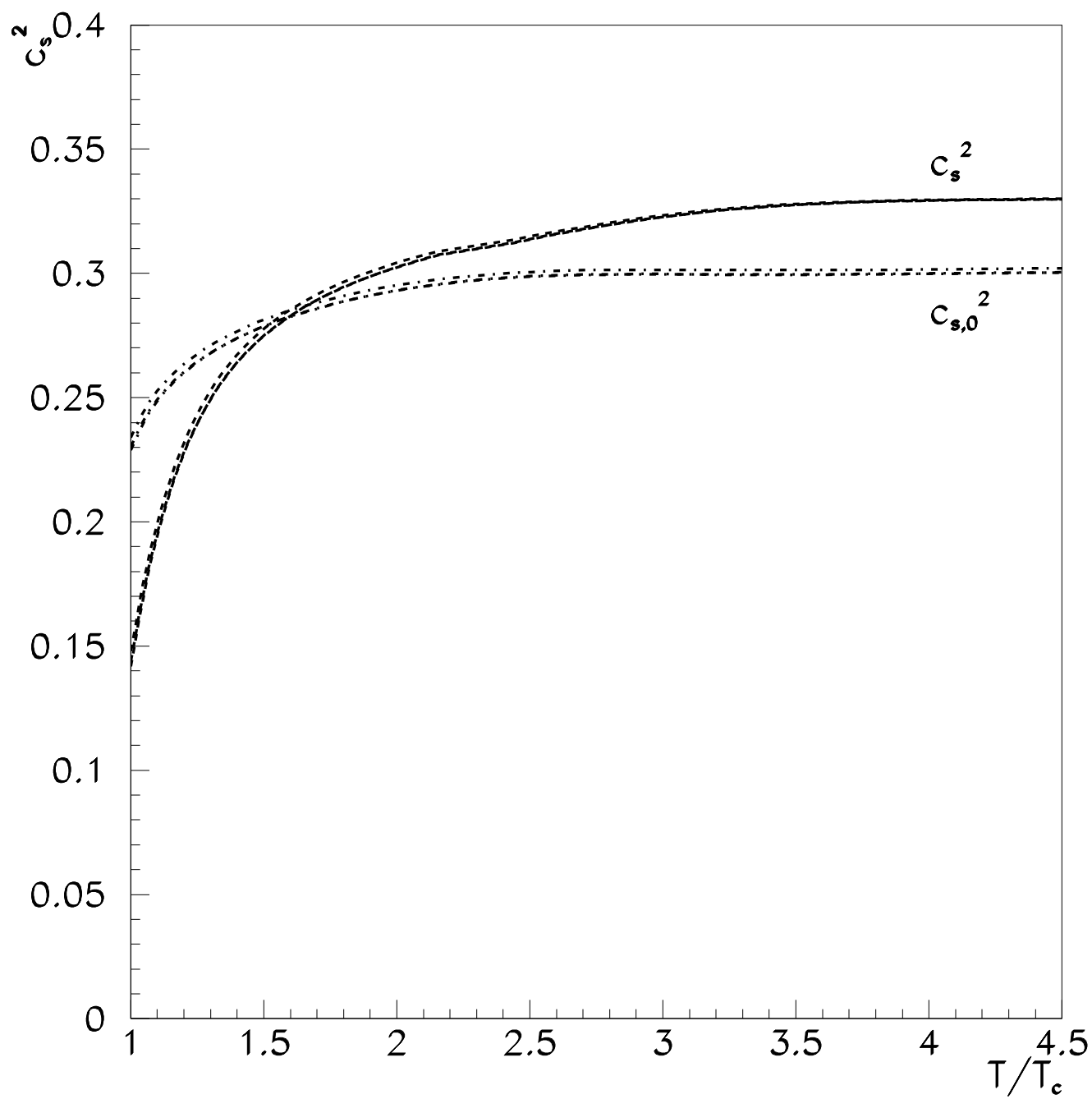


Fig.9. SU(3), $N_f=0,2,4$ --- $M_g(T)$, $M_q(T)$

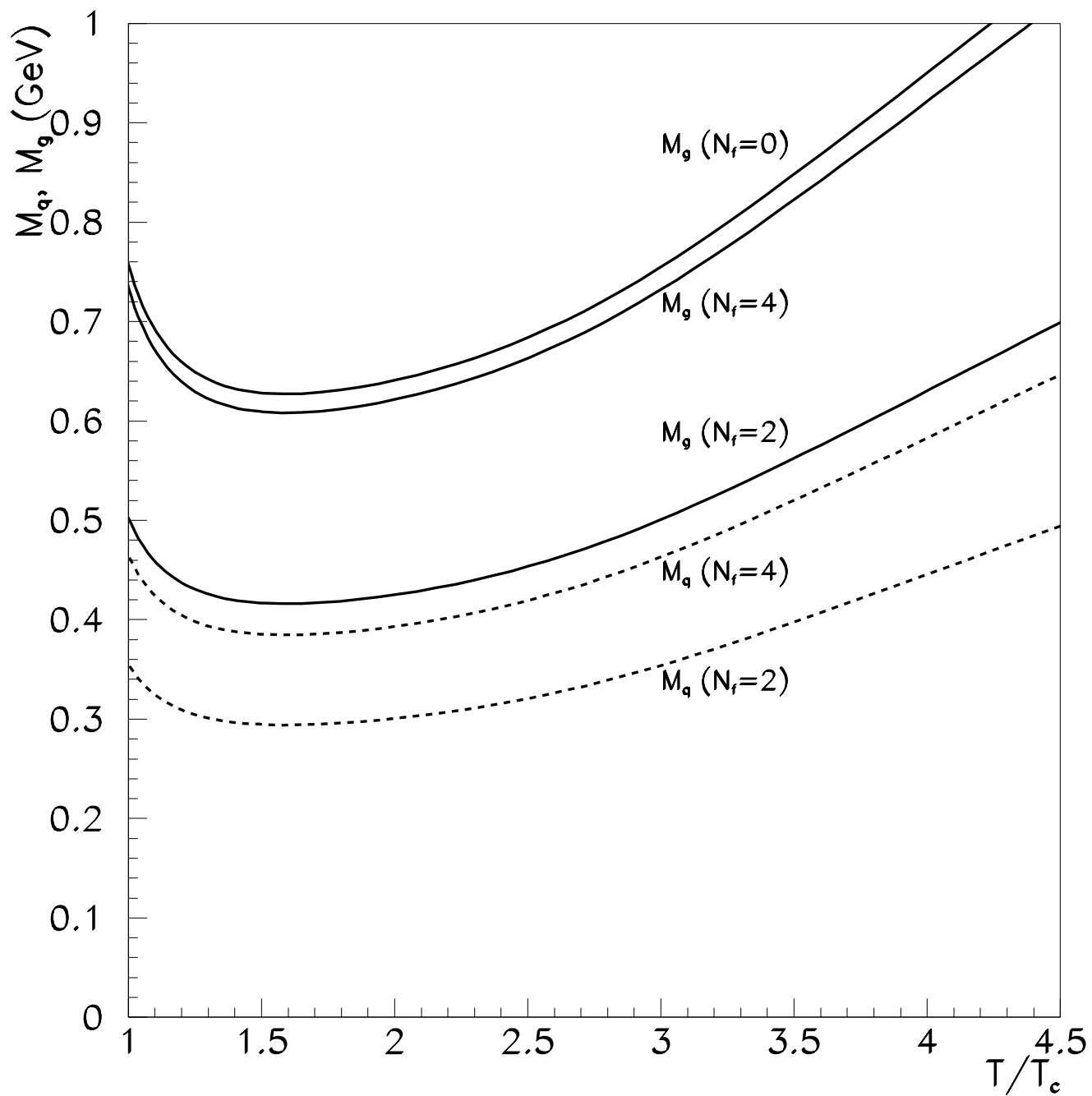


Fig.10. SU(3), $N_f=0,2,4$ --- n_g/n_g^0 , n_q/n_q^0

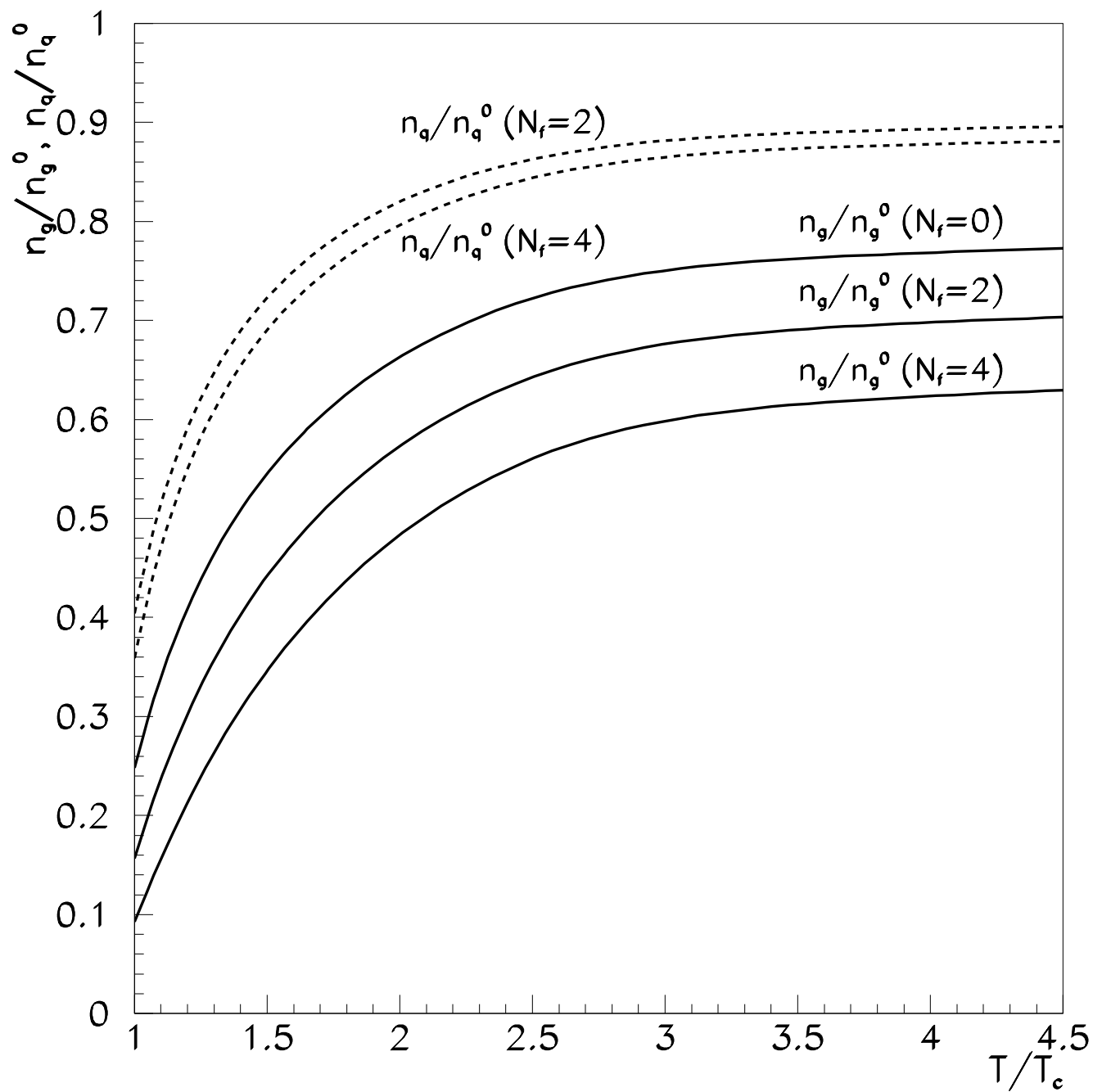


Fig.11. SU(3), $N_f=2,4$ — — $R_g(T)$, $R_g^0(T)$

